

# Gray matter volume of the anterior insular cortex and social networking

Alfredo Spagna<sup>1,2\*</sup>  | Alexander J. Dufford<sup>1\*</sup> | Qiong Wu<sup>3,4\*</sup> | Tingting Wu<sup>1\*</sup> | Weihao Zheng<sup>5</sup> | Edgar E. Coons<sup>6</sup> | Patrick R. Hof<sup>7,8</sup> | Bin Hu<sup>5,9</sup> | Yanhong Wu<sup>3,10</sup> | Jin Fan<sup>1,2,7,8</sup> 

<sup>1</sup>Department of Psychology, Queens College, The City University of New York, New York, New York

<sup>2</sup>Department of Psychiatry, Icahn School of Medicine at Mount Sinai, New York, New York

<sup>3</sup>School of Psychological and Cognitive Sciences, Peking University, Beijing, China

<sup>4</sup>McGovern Institute for Brain Research, Peking University, Beijing, China

<sup>5</sup>School of Information Science and Engineering, Lanzhou University, Lanzhou, China

<sup>6</sup>Department of Psychology, New York University, New York, New York

<sup>7</sup>Fishberg Department of Neuroscience, Icahn School of Medicine at Mount Sinai, New York, New York

<sup>8</sup>Friedman Brain Institute, Icahn School of Medicine at Mount Sinai, New York, New York

<sup>9</sup>CAS Center for Excellence in Brain Science and Intelligence Technology, Shanghai Institutes for Biological Sciences, Chinese Academy of Sciences, Shanghai, China

<sup>10</sup>Beijing Key Laboratory of Behavior and Mental Health, Peking University, Beijing, China

## Correspondence

Jin Fan, Department of Psychology, Queens College, The City University of New York, 65-30 Kissena Blvd., Queens, NY 11367.

Email: jin.fan@qc.cuny.edu

or

Yanhong Wu, Ph.D., School of Psychological and Cognitive Sciences, Peking University, Wusi Road, Haidian, Beijing 100871, China.

Email: wuyh@pku.edu.cn

## Funding information

National Institute of Mental Health (NIMH);

Grant/Award number: MH094305;

National Natural Science Foundation of

China; Grant/Award numbers: 81328008

(to J.F.), 61690205, 31771205 (to Y.W.),

61210010 and 61632014 (to B.H.);

National Key Basic Research and

Development Program of China; Grant/

Award numbers: 2014CB744600 (to B.H.)

and 2015CB351800 (to Y.W.); Program of

Beijing Municipal Science & Technology

Commission; Grant/Award number:

Z171100000117005 (to B.H.); China

Postdoctoral Science Foundation (to Q.W.)

## Abstract

In human life, social context requires the engagement in complex interactions among individuals as the dynamics of social networks. The evolution of the brain as the neurological basis of the mind must be crucial in supporting social networking. Although the relationship between social networking and the amygdala, a small but core region for emotion processing, has been reported, other structures supporting sophisticated social interactions must be involved and need to be identified. In this study, we examined the relationship between morphology of the anterior insular cortex (AIC), a structure involved in basic and high-level cognition, and social networking. Two independent cohorts of individuals (New York group n5 50, Beijing group n5 100) were recruited. Structural magnetic resonance images were acquired and the social network index (SNI), a composite measure summarizing an individual's network diversity, size, and complexity, was measured. The association between morphological features of the AIC, in addition to amygdala, and the SNI was examined. Positive correlations between the measures of the volume as well as sulcal depth of the AIC and the SNI were found in both groups, while a significant positive correlation between the volume of the amygdala and the SNI was only found in the New York group. The converging results from the two groups suggest that the AIC supports network-level social interactions.

## KEYWORDS

anterior insular cortex, amygdala, social networking, surface based morphometry, voxel based morphometry, RRID:SCR\_014196, RRID:SCR\_001847

\*Alfredo Spagna, Alexander J. Dufford, Qiong Wu, and Tingting Wu have contributed equally to this study.

The contents of the present article are solely the responsibility of the authors and do not necessarily represent the official views of funders. The funders had no role in study design, data collection and analysis, decision to publish, or preparation of the manuscript.

## 1 | INTRODUCTION

A social network, that varies in size, complexity, and diversity, is a structure comprised of heterogeneous and nonrandom social interactions among multiple organisms (Croft, James, & Krause, 2008). Compared to other species, social networks of primates are remarkable in their structure and in temporal stability (Shultz & Dunbar, 2007). Living in a large and complex social network has been proposed to be evolutionarily adaptive and the social brain hypothesis states that primates evolved large brains to support complex social systems (Dunbar, 1998). This overall expansion in brain size (Bauernfeind et al., 2013) may reflect increased specialization of specific regions of the brain supporting the rapid and complex processing required by a large social group (Barrett, 2012). A relationship between social network size and complexity and gray matter volume (GMV) in the amygdala, a core region for basic emotion processing (Lewis & Barton, 2006), social-emotional functions (Adolphs, 2010) also related to face processing and associated social significance (Gothard et al., 2018), and its connectivity with prefrontal cortex has been demonstrated (Lewis & Barton, 2006; Bickart, Wright, Dautoff, Dickerson, & Barrett, 2011; Bickart, Hollenbeck, Barrett, & Dickerson, 2012a). However, the cross-species correlations in neocortex volume related to social networking cannot be satisfactorily accounted for only by the volumetrically diminutive amygdala (Dunbar, 2012). That is because successful social networking depends not only on emotional response but also on social cognition, which involves other brain regions and networks (Fan et al., 2011; Von Der Heide, Vyas, & Olson, 2014; Falk & Bassett, 2017). The GMV of a multitude of other frontal and temporal structures has also been associated with social cognition (Kanai, Bahrami, Roylance, & Rees, 2012; Lewis, Rezaie, Br[(20)10(e)23.6(d511.9(23.2(r)-9(L)13.9(e1(a)1b(fr)23.8(&)-369s(ez)204.3(ar)719.3D)20.2(e)26.8(ck)18.4(.8(e)0(r9(L)12(r):)-469.91L)13.9(ev

participants were right-handed. Written informed consent was obtained from each participant. The Institutional Review Boards of the City University of New York and Icahn School of Medicine at Mount Sinai approved the protocol.

For the Beijing group, 100 healthy adults (50 male, 50 female; mean age  $5 21.9$ , SD  $5 2.67$ , range 18–29 years) participated in the study. All participants were right-handed (except for one participant), reported normal or corrected-to-normal vision, and had no known neurological or visual disorders. Participants gave written informed consent in accordance with the procedures and protocols approved by the Human Subjects Review Committee of Peking University. All the procedures performed in this study were in accordance with the ethical standards as laid down in the 1964 Declaration of Helsinki and its later amendments.

## 2.2 | MRI acquisition

For the New York group, T1-weighted images were acquired on a 3 T Siemens Magnetom Skyra MRI scanner with a 16-channel phase-array coil. Foam padding was used to minimize participant head movement and images were acquired along axial planes parallel to the anterior commissure-posterior commissure (AC-PC) line. A high-resolution magnetization prepared rapid gradient-echo (MPRAGE) sequence was used with the following parameters: 176 axial slices each 0.9 mm-thick, skip 5 0 mm, TR 5 2,200 ms, TE 5 2.51 ms, flip angle 5 8°, FOV 5 240 mm, matrix size 5 256 3 256, voxel size 5 0.9 3 0.9 3 0.9 mm. For the Beijing group, the data were acquired on a 3 T Siemens Prisma MRI scanner with a 64-channel phase-array coil. A high-resolution 3D T1 structural image was acquired from each participant using the same sequence with identical parameters as the New York group except the voxel size 5 0.5 3 0.5 3 1 mm. Each T1 image was visually inspected for excessive motion artifact and distortion, and no image was rejected due to these reasons.

## 2.3 | Voxel-based morphometry analyses

Voxel-based morphometry (VBM), a mass-univariate approach, was used to make voxel-wise estimations of the GMV at the first-level of individual participants. The estimated GMV images were then entered into statistical models at the second-level to make group-level statistical inferences (Ashburner & Friston, 2000). In this study, the VBM analyses were conducted using the VBM8 toolbox (RRID:SCR\_014196; <http://dbm.neuro.uni-jena.de/vbm>) and Statistical Parametric Mapping (RRID:SCR\_007037; SPM8, Wellcome Trust Centre for Neuroimaging, University College London, UK) in MATLAB R2012b (RRID:SCR\_001622; Mathworks, Sherborn, MA), following the suggested defaults of the VBM8 manual (RRID:SCR\_014196; <http://dbm.neuro.uni-jena.de/vbm8/VBM8-Manual.pdf>). First, T1-weighted images were segmented into six tissue classes (i.e., gray matter, white matter, cerebrospinal fluid (CSF), bone, nonbrain soft tissue, and air outside of the head and in nose, sinus and ears) using the SPM standard tissue probability map (Mazziotta, Toga, Evans, Fox, & Lancaster, 1995). The DARTEL algorithm (Ashburner, 2007) was used for spatial normalization

of segmented gray matter, white matter, and CSF images, and for resampling of images to 1.5 3 1.5 3 1.5 mm spatial resolution. The modulated normalized images (representing relative volume corrected for brain size) were generated by correcting for nonlinear warping of spatial normalization effect to represent the relative volume after correcting for different brain size. The normalized images were visually inspected for data quality control, and no image showed significant distortion or mis-segmentation for the AIC or the amygdala. Each image was smoothed with a 5-mm full-width-of-half-maximum (FWHM) Gaussian kernel. The identical analysis pipeline was applied to the images from the two cohorts.

## 2.4 | Surface-based morphometry analyses

Cortical surface reconstruction was performed using FreeSurfer version 5.3 and visualized using FreeSurfer version 6 (RRID:SCR\_001847; <http://surfer.nmr.mgh.harvard.edu>), following pre-processing pipelines of previous publications (Dale, Fischl, & Sereno, 1999; Fischl, Sereno, & Dale, 1999; Fischl & Dale, 2000; Fischl, Liu, & Dale, 2001). Briefly, pre-processing steps included motion correction, removal of non-brain tissue (Ségonne et al., 2004), automated Talairach transformation, intensity normalization, segmentation of subcortical structures, generation of grey/white matter interface via volume tessellation and deformation (Dale et al., 1999). Topology and geometry of the reconstructed surface were then validated once the cortical surface reconstruction was complete (Fischl et al., 2001). The reconstructed images were visually inspected using FreeView and segmentation errors, including correction of non-brain tissue, missing white matter, and errant grey matter, were manually corrected (<http://sites.bu.edu/cnrlab/lab-resources/freesurfer-quality-control-guide>). Further data processing included surface inflation, registration to average spherical atlas (Fischl et al., 1999), and calculation of surface measurements that included cortical thickness (CT), surface area (SA), volume (VOL), local gyrification index (LGI), and sulcal depth (SD). CT is a measure of the distance between gray and white matter surface at each vertex (Fischl & Dale, 2000). SA is the averaged area of surrounding triangles of a vertex. For cortical regions, VOL is the product of CT and SA, which is similar, but not identical, to GMV in VBM. For the subcortical regions, VOL could only be measured as voxels count in a predefined region of interest (ROI), which is not recommended by FreeSurfer (RRID:SCR\_001847). Therefore, the VOL was not used to examine the subcortical regions (i.e., amygdala) and was applied only to the cortical regions. LGI is the ratio of cortical folding to convex hull surface area (Schaer et al., 2008, 2012). SD is the integrated dot product of the movement vector with a normal surface measures, which measures both the distances upward and downward to the average surface (Fischl et al., 1999; Destrieux, Fischl, Dale, & Halgren, 2010). All imaging data were smoothed with a 10-mm FWHM Gaussian kernel.

## 2.5 | Social network measures

A composite measure of the SNI (Cohen, Doyle, Skoner, Rabin, & Gwaltney, 1997a), which quantifies three indices of a participant's social network: network diversity, social network size, and number of

embedded networks, was used in this study. For all indices, the SNI criteria define a high contact role as a person with whom the respondent interacts at least once every 2 weeks. The network diversity index of the SNI measures the number of high contact roles from 12 possible social roles (e.g., spouse, relative, church member, classmate) in which a score of 1 is assigned if the respondent has at least one member in that group who is considered a high contact role. Network diversity score is an integer value ranging from 0 to 12 with a greater score indicating higher social network diversity. The social network size index is the total number of high contact people across each of the 12 roles and provides an aggregate estimate of the respondent's total network size, with a greater score indicating larger total social network size. Network complexity (synonymous with the number of embedded networks) is the number of network domains, ranging from 0 to 8, in which the respondent is active at a criterion level of 4 or more high-contact roles, providing a quantification of the extent of complexity in the respondent's social network. The eight network domains include family, friends, church/temple, school, work, neighbors, volunteering, and "other groups." Respondents had the opportunity to write in social groups that are part of their network but are not explicitly listed as part of the index in the "other group" domain (i.e., a Boy Scout troop or a sports team). The "other group" scores were treated as an additional domain and scored accordingly for the quantification of each index.

Due to that the three indexes of network diversity, social network size, and number of embedded networks are calculated from participants' responses to the same twelve items, we conducted factor analysis to identify whether the three variables are associated with one or more latent variables. Results for the New York group showed that a latent variable (i.e., the composite SNI score used) explained 82.41% of the variance, while a second factor explained 12.03% and a third factor explained 5.56% of the variance. Because only one component was extracted, no rotation was possible. Factor loading results showed that the normalized network complexity score was the largest factor loading (0.94), followed by the normalized network size (0.91), and normalized network diversity scores (0.88). Therefore, a composite SNI score was calculated for each participant, by first standardizing and then averaging the three scores. Reliability statistics of the composite SNI score, in terms of Cronbach's  $\alpha$ , was 0.89, suggesting that the items had a relatively high internal consistency (Cronbach's  $\alpha$  before standardization was 0.53).

For the Beijing group, we replicated results of the New York group in terms of factor analysis and reliability. Specifically, results showed that a latent variable (i.e., the composite SNI score used) explained 83.83% of the variance, while a second factor explained 13.14% and a third factor explained 3.03% of the variance. Factor loading results showed that the normalized network complexity score was the largest factor loading (0.96), followed by the normalized network size (0.93), and normalized network diversity scores (0.85). The composite SNI score was calculated in the same way as in the New York group. Reliability statistics of the composite SNI score, in terms of Cronbach's  $\alpha$ , was 0.90 suggesting that the items had a relatively high internal consistency (Cronbach's  $\alpha$  before standardization was 0.60). Gender

differences in terms of SNI were also examined in the two samples using two-tailed independent sample t tests.

The IQ of participants from the New York group was measured using three subtests (Vocabulary, Figure Weights, and Symbol Search) of the Wechsler Adult Intelligence Scale (WAIS) (Wechsler, 2014). We examined the relationship between the composite SNI score and IQ in the New York group to investigate the potential contribution of intellectual ability to individual's social networking.

## 2.6 | Correlation and regression analyses

For the VBM, smoothed GMV images from all participants were entered into a random-effects general linear model (GLM) for the second-level group analysis, with the composite SNI scores across all participants as the predictor. An absolute threshold mask of 0.1 was used for all the second-level analyses to exclude noise signals outside the brain. This GLM was  $.7(m)0M1ore$

To illustrate the GMV-SNI association in AIC and amygdala, we conducted ROI analyses. The ROI of the right AIC was defined as the cluster showing significant positive main effect of SNI, while the ROI of left AIC, left amygdala, and right amygdala were defined as the clusters showing significant positive group by SNI interaction effect. Here we did not use the anatomically defined ROI, because we did not have an assumption that the GMV of all voxels in the AIC and amygdala would be homogeneously associated with the SNI. For each ROI, the first eigenvariate of the GMV value was extracted across all voxels within the corresponding cluster from the GMV image for each participant. The scatter plot of the GMV-SNI association was generated for each region in each group.

For the surface-based morphometry analyses, Pearson correlations between each surface measure of cortical vertices and composite SNI measure across participants were calculated. The bilateral AIC mask was created according to the literature (Fan et al., 2016). Similar to the VBM analysis, a significance level for the height of each vertex as  $p < .05$  was applied, together with an estimated extent threshold to correct for the multiple comparisons across vertices in the AIC, resulting in a corrected threshold as  $p < .05$ . To estimate the extent threshold, the vertices in each ROI were transformed back to the MNI voxel space. The extent threshold was then estimated using AlphaSim. For cortical regions outside the AIC mask, false discovery rate (FDR) correction of  $p < .05$  was applied.

### 3 | RESULTS

Results from the VBM analyses of the New York group (Figure 1a,b) showed a positive correlation between GMV and the composite SNI score in the left AIC (local peak:  $x = 2, y = 39, z = 8$ , and  $T = 2.93$ ,  $Z = 2.79$ ; cluster size  $k = 294 > \text{extent threshold} = 204$ ), in addition to the right amygdala ( $x = 22, y = 4, z = 21$ , and  $T = 2.72$ ,  $Z = 2.61$ ;  $k = 53 > \text{extent threshold} = 40$ ). When mean white matter volume, mean CSF volume, age and gender were included as the nuisance regressors in the GLM, the correlation between the GMV of the left AIC and the SNI score was still significant ( $x = 2, y = 6, z = 9$ , and  $T = 3.29$ ,  $Z = 3.09$ ;  $k = 640$ ), while the correlation between the right amygdala and the SNI was not significant ( $x = 22, y = 4, z = 21$ , and  $T = 2.36$ ,  $Z = 2.28$ ;  $k = 12$ ). For the whole-brain exploratory analyses with conservative threshold ( $FWE < .05$ ), no voxel or cluster inside or outside the masks of AIC and amygdala showed significant correlation between the SNI scores and the GMV.

Results from the VBM analyses of the Beijing group (Figure 1c,d) showed a positive correlation between GMV of the right AIC and the composite SNI score ( $x = 34, y = 18, z = 7$ , and  $T = 2.93$ ,  $Z = 2.86$ ;  $k = 262 > \text{extent threshold} = 233$ ), while no significant correlation was found between the GMV of the amygdala and the SNI score (no cluster passed the extent threshold  $= 42$ ). When gender and age were included as the nuisance regressors in the GLM, the correlation between the GMV in the right AIC and the SNI score was still significant ( $x = 34, y = 18, z = 7$ , and  $T = 2.92$ ,  $Z = 2.85$ ;  $k = 281$ ), while the correlation between the GMV of the amygdala and the SNI was not

significant. No significant correlation was found between the GMV and SNI scores for areas inside or outside the masks of AIC and amygdala.

Results from the GLM analysis of VBM with both New York and Beijing groups included (Figure 2a,b) showed a positive correlation between GMV and SNI (the main effect of SNI) in right AIC ( $x = 38, y = 10, z = 12$ , and  $T = 2.48$ ,  $Z = 2.45$ ;  $k = 380 > \text{extent threshold} = 223$ ), while this main effect was not significant in the amygdala. The positive SNI by group interaction was found in the left AIC ( $x = 2, y = 8, z = 6$ , and  $T = 3.45$ ,  $Z = 3.38$ ;  $k = 261 > \text{extent threshold} = 223$ ), and in the right amygdala ( $x = 22, y = 3, z = 21$ ; and  $T = 3.52$ ,  $Z = 3.44$ ;  $k = 166 > \text{extent threshold} = 164$ ), while no negative interaction effect was found either in the AIC or the amygdala. No significant main effect or interaction effect was found for areas inside or outside the masks of AIC and amygdala. The scatter plot of the correlation between GMV and SNI for each ROI is shown in Figure 3.

Results from the surface-based morphometry (SBM) analyses of the New York group (Figure 4a) showed a positive correlation between the SNI scores and the VOL of the left AIC ( $x = 2, y = 10, z = 5$ , and  $r = .40$ ,  $p = .0041$ ;  $k = 55 > \text{extent threshold} = 37$ ), SD of the right AIC ( $x = 42, y = 1, z = 2$ ;  $r = .42$ ,  $p = .0025$ ;  $k = 49 > \text{extent threshold} = 38$ ), and SA of the left AIC ( $x = 2, y = 17, z = 9$ ;  $r = .42$ ,  $p = .0023$ ;  $k = 39 > \text{extent threshold} = 31$ ). No significant correlation was found between the CT or LGI in any vertex of the AIC and the composite SNI score. For other regions outside the AIC mask, no significant correlation was found for any surface-based measurement.

Results from the SBM analyses of the Beijing group (Figure 4b) showed a positive correlation between the SNI scores and the SD of the right AIC ( $x = 34, y = 17, z = 9$  and  $r = .33$ ,  $p = .0023$ ;  $k = 28 > \text{extent threshold} = 24$ ). No significant correlation was found between the other surface-based measurements in any vertex of the AIC and the composite SNI scores. For other regions outside the AIC mask, no significant correlation was found for any surface-based measurement.

The Pearson's correlation coefficient between IQ and SNI in the New York group was not significant ( $r = .08$ ,  $p = .55$ , two-tailed). No significant gender differences were found for both the New York group, ( $t_{(48)} = 0.24$ ,  $p = .81$ ), and for the Beijing group ( $t_{(98)} = 0.49$ ,  $p < .62$ ) on the composite SNI score.

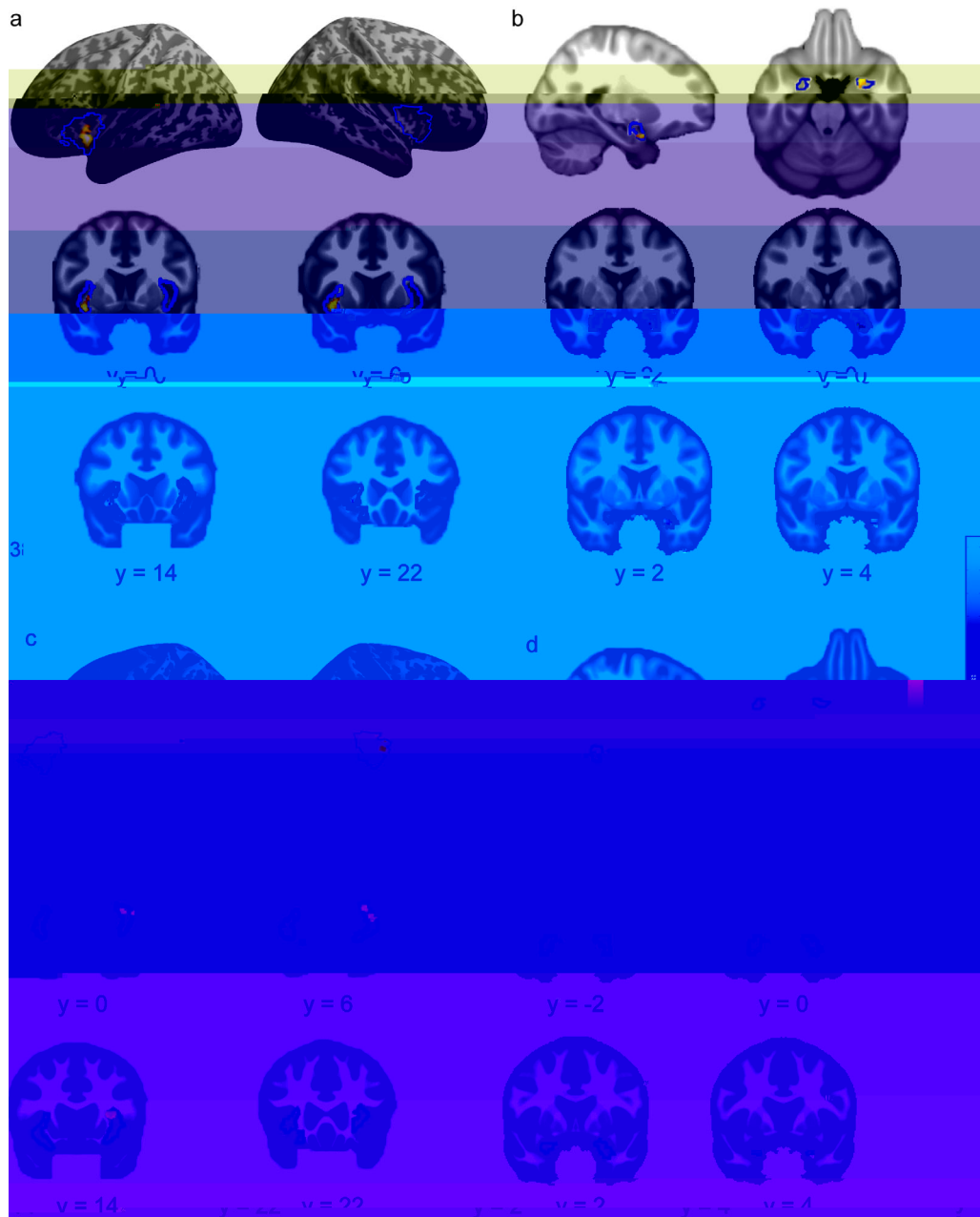


**FIGURE 1** Results of the voxel-based analyses for the association between GMV and SNI score in the New York group for the AIC (a) and amygdala (b) and in the Beijing group for the AIC (c) and amygdala (d). Blue contours indicate the boundary of the anatomically defined masks of AIC and amygdala. The color bar indicates the coding of the statistical T values in the color map, with brighter color for greater T values [Color figure can be viewed at [wileyonlinelibrary.com](http://wileyonlinelibrary.com)]

environments (Bauernfeind et al., 2013) and therefore it could potentially account for some of the variance in cross-species correlations in brain size related to social network complexity observed across evolution (Bauernfeind et al., 2013).

The relationship between function and structure of the brain is a longstanding question in neuroscience, as development phases and expansion of the central nervous system do not follow a geometrically linear similarity across mammals, and with structural changes further differing across brain lobes in humans (Hofman, 2014). The AIC, located in the depth of the lateral sulcus, is a structure related to the

frontal lobe. It follows a linear pathway of cortical maturity (i.e., thinning) from adolescence to adulthood (Shaw et al., 2008) and these changes are associated with a more adult-like behavior (i.e., less risky decision-making) (Smith, Steinberg, & Chein, 2014). A successful transition from adolescence to adulthood requires the acquisition and implementation of socially appropriate behavior, learned through peer-to-peer interactions and social exclusions (Kilford, Garrett, & Blakemore, 2016), and this psychologically critical period is connoted by structural changes, in the form of hierarchical organization and expansion of axonal mass allowing local and global communication

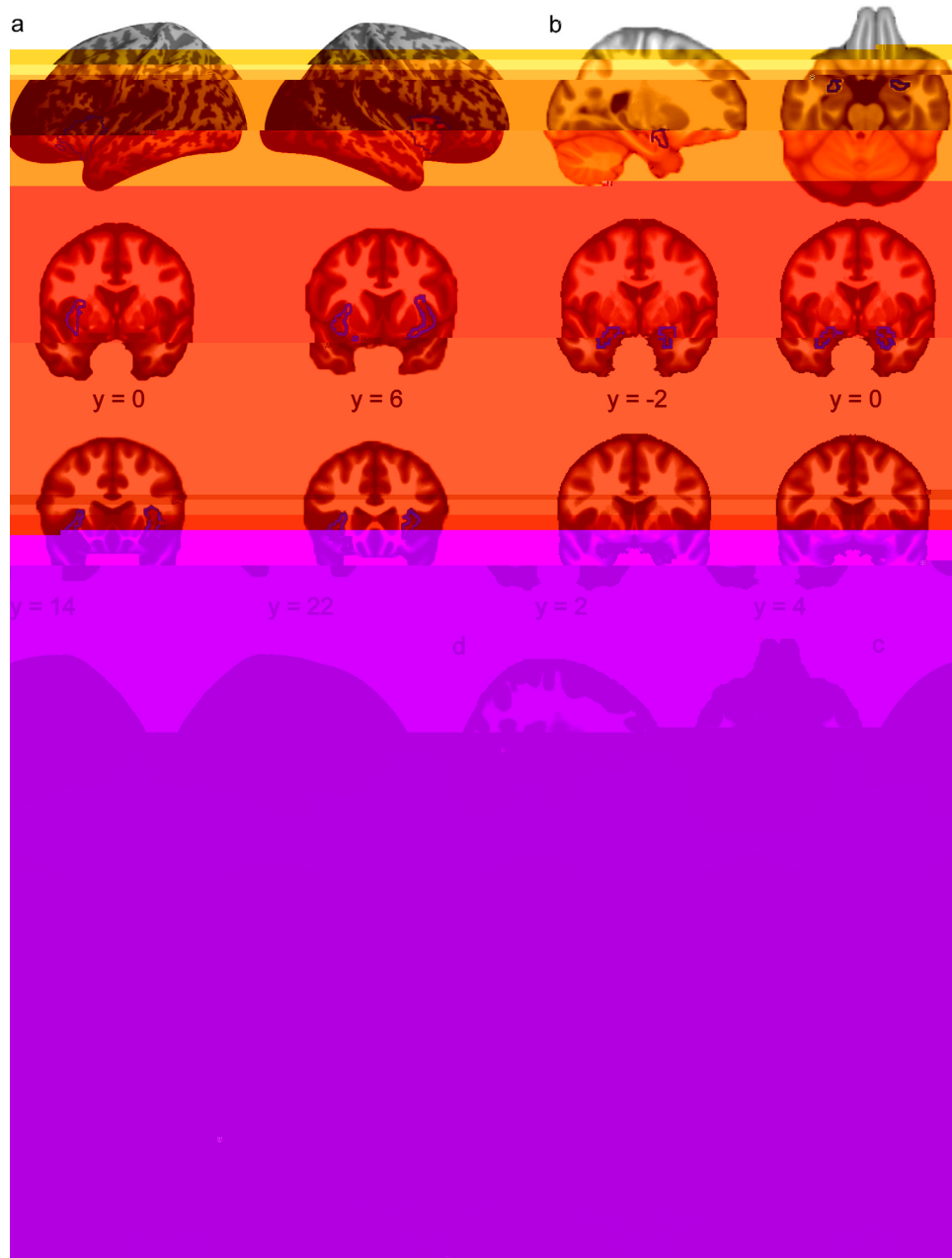


**FIGURE 2** Main effect of the association between the GMV and SNI in the AIC (a) and amygdala (b), and the group by SNI association

(Hofman, 2014), especially in areas within the frontal lobe that are critical for emotion-cognition interaction (Gu, Liu, Van Dam, Hof, & Fan, 2013b) and for cognitive control and self-regulation (Hofmann, Schmeichel, & Baddeley, 2012). Although the current study did not embrace a developmental perspective, we argue that our result may add new evidence regarding the relationship between function and structure of the AIC, indicating that, in line with the “bigger is better hypothesis” proposed by Hofman (2014), an expansion of the surface of the AIC supports an expansion of social interactions of individuals at the network level.

Along with morphological evidence showing that the AIC could be involved in social cognition also at the group level, activation in the AIC has been shown in a variety (and somehow strikingly different) of cognitive functions, ranging from the implementation of bottom-up detection of salient events and coupling with the anterior cingulate cortex (ACC) for rapid access to motor response (i.e., the salience network; Menon & Uddin, 2010) and to top-down cognitive control (i.e., the cingulo-opercular network—CON; Dosenbach, Cohen, Schlaggar, & Petersen, 2008; Wu et al., 2017). Behaving appropriately in a human social network does not only require the processing of sensory



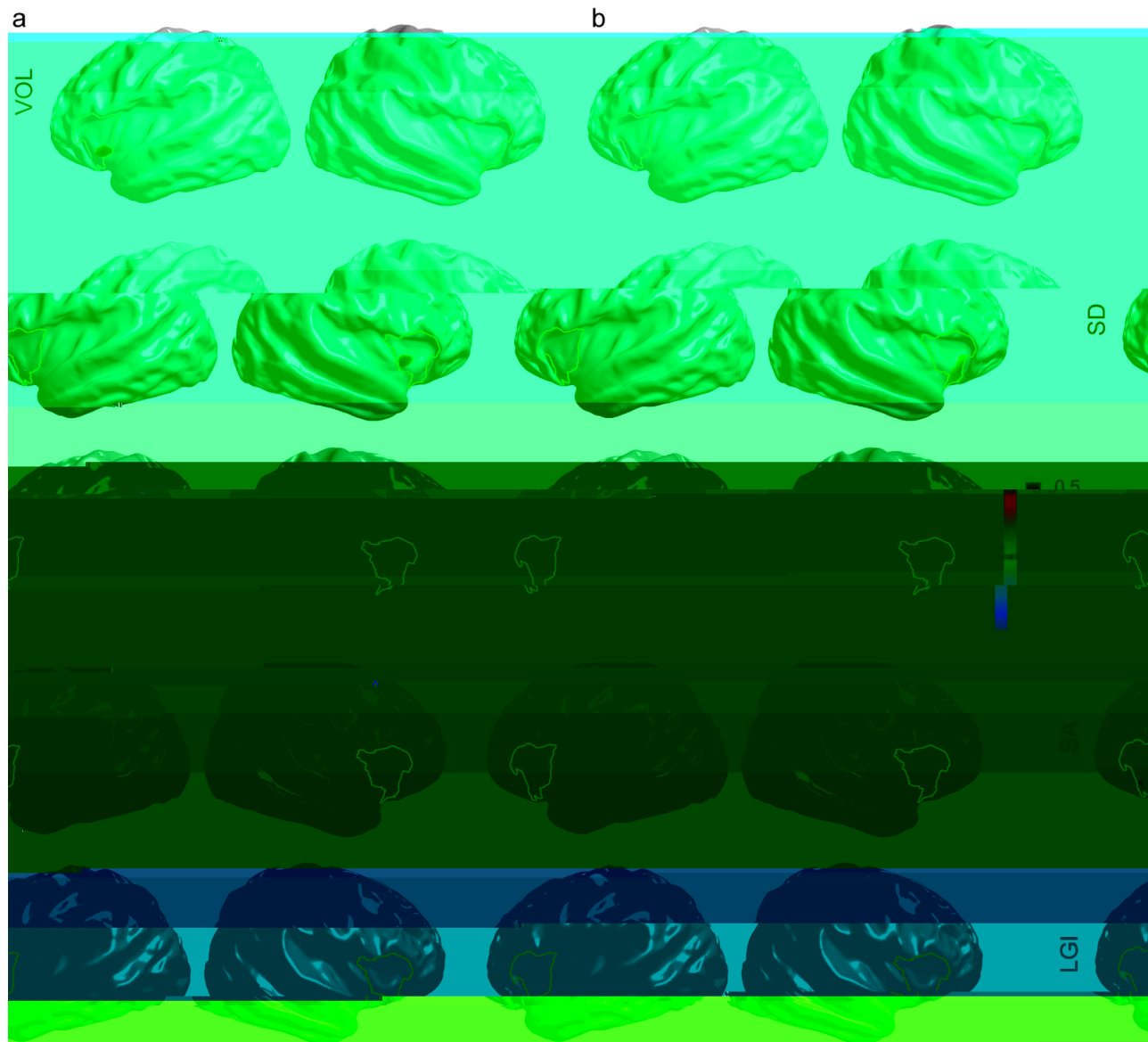


**FIGURE 4** Surface-based analyses for the association between morphological features and SNI score in the New York group (a) and in the Beijing group (b). Green contours indicate the boundary of the anatomically defined mask of AIC used in this study. VOL 5 volume; SD 5 sulcal depth; CT 5 cortical thickness; SA 5 surface area; LGI 5 local gyrification index. The color bar indicates the coding of the magnitude of Pearson's  $r$  values in the color map, with warm colors for positive  $r$  values and cold colors for negative  $r$  values [Color figure can be viewed at [wileyonlinelibrary.com](http://wileyonlinelibrary.com)]

was in the left AIC while the significance of the GMV - SNI correlations for the Beijing group was in the right AIC (the result of the interaction). A potential explanation for this difference may be related to differences in language-related processing between the Chinese (logographic) and the English (alphabetic). This suggests a lateralization of the AIC, which is a key region for language and speech processing (Ardila, Bernal, & Rosselli, 2014; Oh, Duerden, & Pang, 2014) and the reported hemispheric dominance of aspects of language across cultures (Tzeng, Hung, Chen, Wu, & Hsi, 1986; Chen, 1993; Cao, Kim, Liu, & Liu, 2014). Therefore, the right- vs left-lateralized GMV-to-SNI association shown in the VBM (but not firmly confirmed by the surface-based morphometry analyses) may be language-specific rather than related to the social-network per se. Future studies are warranted further to explore the

impact of culture on social networking and the brain structures involved.

Some limitations of the present study should be however kept in mind. First, correlational analyses do not provide causative evidence. Although this study shows that social networking is correlated with morphological features in the AIC, it cannot be concluded that increased social network results from increases in the GMV of the AIC or vice versa. Second, in line with the existence of between-group differences, a potential limitation may reside in the use of an adapted version from English to Chinese of the Social Network Index, with the translation being conducted by three Chinese authors of this manuscript (J.F., T.W., Q.W.). Although translation reliability was independently assessed by the authors, and with the consistency of the

translated questionnaire being demonstrated by the reliability analyses, the cross-cultural dependence of some items of the Social Network Index may have influenced the measure of the SNI.

#### **ACKNOWLEDGMENTS**

Central to the initiation of this study, along with JF and EEC, was the anthropologist Dr. Graham Pringle. Sadly, he would also have been an author of this study's report but for his sudden death before he could participate in its written formulation and critical review.

#### **CONFLICT OF INTEREST**

The authors declare no conflict of interest.

#### **AUTHOR CONTRIBUTIONS**

J.F., A.D., G.P., and E.E.C. designed the study. A.D. and Q.W. collected the data. A.D., Q.W., T.W., and Z.W. analyzed the data with assistance from J.F., A.S., A.D., J.F., P.R.H., Q.W., T.W., E.C., T.N., and Y.W. wrote the paper.

#### **ORCID**

Alfredo Spagna  <http://orcid.org/0000-0001-5170-0320>

Jin Fan  <http://orcid.org/0000-0001-9630-8330>

#### **REFERENCES**

Adolphs, R. (1999). Social cognition and the human brain. *Trends in Cognitive Sciences*

Craig  
an  
Croft,  
won  
Dale, A  
ana  
(2),  
Destri  
lat  
no  
Dose  
(2)  
C  
Dun  
Dun  
Ec  
F

- control network subserving diverse executive functions. *Cognitive, Affective, & Behavioral Neuroscience* 12(2), 241–268.
- Odriozola, P., Uddin, L. Q., Lynch, C. J., Kochalka, J., Chen, T., & Menon, V. (2016). Insula response and connectivity during social and non-social attention in children with autism. *Social Cognitive and Affective Neuroscience* 11(3), 433–444.
- Oh, A., Duerden, E. G., & Pang, E. W. (2014). The role of the insula in speech and language processing. *Brain and Language* 135, 96–103.
- Raichle, M. E. (2015). The brain's default mode network. *Annual Review of Neuroscience* 38, 433–447.
- Robinson, J. L., Laird, A. R., Glahn, D. C., Lovallo, W. R., & Fox, P. T. (2010). Metaanalytic connectivity modeling: Delineating the functional connectivity of the human amygdala. *Human Brain Mapping* 31(2), 173–184.
- Rosati, A. G. (2017). Foraging cognition: Reviving the ecological intelligence hypothesis. *Trends in Cognitive Sciences* 21(9), 691–702.
- Sadaghiani, S., & D'Esposito, M. (2015). Functional characterization of the cingulo-opercular network in the maintenance of tonic alertness. *Cerebral Cortex (New York, N.Y.: 1991)* 25(9), 2763–2773.
- Sallet, J., Mars, R. B., Noonan, M., Andersson, J. L., O'Reilly, J., Jbabdi, S., ... Rushworth, M. F. (2011). Social network size affects neural

